

ARTICLE

Received 3 Dec 2013 | Accepted 15 Apr 2014 | Published 2 Jun 2014

DOI: 10.1038/ncomms4904

Transient expression of Bcl6 is sufficient for oncogenic function and induction of mature B-cell lymphoma

Michael R. Green^{1,*}, Carolina Vicente-Dueñas^{2,3,*}, Isabel Romero-Camarero^{2,3}, Chih Long Liu¹, Bo Dai¹, Inés González-Herrero^{2,3}, Idoia García-Ramírez^{2,3}, Esther Alonso-Escudero^{2,3}, Javeed Iqbal⁴, Wing C. Chan⁴, Elena Campos-Sanchez⁵, Alberto Orfao⁶, Belén Pintado⁷, Teresa Flores^{3,8}, Oscar Blanco⁸, Rafael Jiménez^{3,9}, Jose Angel Martínez-Climent¹⁰, Francisco Javier García Criado¹¹, María Begoña García Cenador¹¹, Shuchun Zhao¹², Yasodha Natkunam¹², Izidore S. Lossos¹³, Ravindra Majeti¹, Ari Melnick¹⁴, César Cobaleda⁵, Ash A. Alizadeh^{1,*} & Isidro Sánchez-García^{2,3,*}

Diffuse large B-cell lymphoma (DLBCL) is the most common lymphoma and can be separated into two subtypes based upon molecular features with similarities to germinal centre B-cells (GCB-like) or activated B-cells (ABC-like). Here we identify gain of 3q27.2 as being significantly associated with adverse outcome in DLBCL and linked with the ABC-like subtype. This lesion includes the *BCL6* oncogene, but does not alter *BCL6* transcript levels or target-gene repression. Separately, we identify expression of *BCL6* in a subset of human haematopoietic stem/progenitor cells (HSPCs). We therefore hypothesize that *BCL6* may act by 'hit-and-run' oncogenesis. We model this hit-and-run mechanism by transiently expressing *Bcl6* within murine HSPCs, and find that it causes mature B-cell lymphomas that lack Bcl6 expression and target-gene repression, are transcriptionally similar to post-GCB cells, and show epigenetic changes that are conserved from HSPCs to mature B-cells. Together, these results suggest that *BCL6* may function in a 'hit-and-run' role in lymphomagenesis.

¹ Divisions of Oncology and Hematology, Department of Medicine, School of Medicine, Stanford University, Stanford, California 94305, USA. ² Experimental Therapeutics and Translational Oncology Program, Instituto de Biología Molecular y Celular del Cáncer, CSIC/Universidad de Salamanca, Campus M. de Unamuno s/n, 37007 Salamanca, Spain. ³ Institute of Biomedical Research of Salamanca (IBSAL), 37007 Salamanca, Spain. ⁴ Department of Pathology and Microbiology, University of Nebraska Medical Center, Omaha, Nebraska 68198, USA. ⁵ Centro de Biología Molecular Severo Ochoa, CSIC/Universidad Autónoma de Madrid, c/Nicolás Cabrera, nº 1, Campus de Cantoblanco, 28049 Madrid, Spain. ⁶ Servicio de Citometría and Departamento de Medicina, Universidad de Salamanca, 37007 Salamanca, Spain. ⁷ Genetically Engineered Mouse Facility, CNB-CSIC, 28006 Madrid, Spain. ⁸ Departamento de Anatomía Patológica, Universidad de Salamanca, 37007 Salamanca, Spain. ⁹ Departamento de Fisiología y Farmacología, Universidad de Salamanca, Campus M. Unamuno s/n, 37007 Salamanca, Spain. ¹⁰ Division of Oncology, Center for Applied Medical Research (CIMA), University of Navarra, 31008 Pamplona, Spain. ¹¹ Departamento de Cirugía, Universidad de Salamanca, 37007 Salamanca, Spain. ¹² Department of Pathology, Stanford University School of Medicine, Stanford, California, 94305 USA. ¹³ Division of Hematology-Oncology, University of Miami, Sylvester Comprehensive Cancer Center, Miami, Florida 33136, USA. ¹⁴ Departments of Medicine and Pharmacology, Weill Cornell Medical College, New York, New York 10021, USA. * These authors contributed equally to this work. Correspondence and requests for materials should be addressed to A.A.A. (email: arasha@stanford.edu) or to I.S.-G. (email: isg@usal.es).

As the most common aggressive lymphoma afflicting nearly 30,000 Americans each year, diffuse large B-cell lymphoma (DLBCL) is highly heterogeneous. Current combination therapeutic regimens typically fail in nearly half of all patients with DLBCL, many of whom succumb to their disease. Given the inability to cure many patients with DLBCL, and the significant toxicity of current therapies, better treatment strategies are needed. We previously described a major molecular determinant of this biological and clinical heterogeneity, likely reflecting the cellular origin of tumours. Patients with tumours that have transcriptional profiles related to germinal centre B-cells (GCB-like) have a better overall survival than those with tumours having a transcriptional profile related to post-GCB-activated B-cells (ABC-like)¹. This finding has been validated by several groups independently, and the molecular basis for this diversity in DLBCL has been partially deciphered in studies of distinctive genomic aberrations and somatic mutations in DLBCL subtypes.

Genomic studies have defined a subset of alterations that stratify between the two DLBCL subtypes^{2,3}, with point mutations of histone-modifying genes and B-cell receptor signalling components as the prevailing dominant drivers or accelerators of the disease⁴. However, these alterations are found in only a fraction of patients, and the relationship between more common genetic alterations and DLBCL subtypes remains largely obscure. For example, the most frequent somatic alteration observed in DLBCL, involving genetic translocation of *BCL6*, is arguably the most prominent and paradoxical^{5,6}. *BCL6* is a central regulator of germinal centre development^{7,8}, is more highly expressed in the GCB-like subtype of DLBCL compared with the ABC-like subtype; and is associated with a favourable prognosis^{1,9}. Yet genetic translocations of this gene are more prominent in the post-GCB subtype of the disease and are associated with adverse outcome^{1,10}. Recent findings have implicated *BCL6* in leukaemia stem cell survival^{11,12}, and show that its activity may be altered by *CREBBP* or *EP300* mutation³ at an early-stage lymphoma development^{13,14}. Separately, genetic and epigenetic aberrations in premalignant haematopoietic progenitors have recently been described in several haematological malignancies, including acute myeloid leukemia and chronic lymphocytic leukemia^{15–18}. Together, these findings led us to postulate that *BCL6* may promote tumorigenesis in a manner contrasting that of other traditional oncogenes that act in fully evolved tumour cells and require persistent activity due to oncogene addiction¹⁹.

Somatic DNA copy number alterations (SCNAs) perturb more of the cancer genome than any other somatic alteration, and can alter the gene dosage and subsequent expression of multiple genes in a single alteration²⁰. The significance of SCNAs can be assessed from the patterns of broad and focal gains/losses across the genomes of a tumour cohort, allowing potential target genes within conserved regions of DNA copy number gain/loss to be identified. The integration of expression profiling data has additionally allowed putative driver genes within each lesion to be localized by their changes in transcript abundance resulting from altered gene dosage²¹. However, a subset of oncogenes with negative feedback loops may act in a 'hit-and-run' fashion; therein, transient expression of the oncogene may induce broad changes to the cancer genome, epigenome or transcriptome, and be sufficient for oncogenesis in the absence of persistent expression. These 'hit-and-run' oncogenes may therefore not be detected by integrative analysis of DNA copy number and gene expression changes, and are difficult to identify in the absence of other genetic alterations targeting the same locus, such as genetic translocations or somatic mutations.

Here we use high-resolution analysis of DNA copy number across a large cohort of DLBCL tumours to elucidate recurrent alterations in this disease. We identify gain of the *BCL6* oncogene

as being a potential 'hit-and-run' oncogene associated with poor outcome and the ABC-like DLBCL subtype. Using transgenic mouse models, we confirm that transient expression of *Bcl6* is sufficient to induce aggressive mature B-cell lymphoma that appears transcriptionally similar to activated post-GCB cells.

Results

Gain of 3q27.2 is associated with inferior outcome in DLBCL. Using high-resolution DNA copy number profiles of 609 DLBCL tumours analysed using the Genomic Identification of Significant Targets in Cancer (GISTIC) method, we mapped the landscape of SCNAs in this disease. We identified 22 peaks of significant DNA copy number loss (GISTIC, *Q* value <0.25) and 17 peaks of significant DNA copy number gain (Fig. 1a and Supplementary Table 1). We analysed the association of each lesion with overall survival in cohorts of patients treated with combination chemotherapy (cyclophosphamide, adriamycin, vincristine, prednisone [CHOP], *n* = 232) or in combination with Rituximab (R-CHOP, *n* = 196). Gain of 3q27.2 was the most prognostic lesion and was associated with significantly decreased overall survival in both cohorts (Fig. 1b,c and Supplementary Table 1). For 249 cases, matched gene expression profiling data was available and allowed for classification of samples into GCB-like and ABC-like subtypes using the previously defined method (Fig. 1d). Gain of 3q27.2 was significantly over-represented in the ABC-like DLBCL subtype (Fisher *P* value = 8.1×10^{-8}), suggesting that it may contribute to the genetic aetiology of this subtype and its association with adverse outcome.

The peak of this alteration (chr3:180478352-199501827) contained 134 genes, including the lymphoma oncogene *BCL6* (ref. 22), but not a previously hypothesized target of chromosome 3 alterations, *FOXP1* (ref. 23); Fig. 2a). The significance of the 3q27.2 peak resulted from a combination of broad events (trisomy 3 and 3q arm-level gain) and recurrent focal gains of 3q27.2 over the *BCL6* locus (Fig. 2b). Furthermore, 3q27.2 DNA copy number gains were mutually exclusive of translocations targeting *BCL6* in the 48 tumours for which such data were available²⁴, suggesting that *BCL6* is a likely target of these lesions (Fig. 2b). However, there was no significant increase in either *BCL6* expression or target gene²⁵ repression in cases with 3q27.2 gain compared with those cases with diploid copy number (Fig. 2c,d). This same trend was also observed within the context of *BCL6* translocations (Fig. 2e,f), as previously described¹⁰. The absence of increased *BCL6* transcript levels in tumours harbouring these genomic alterations could not be attributed to the uniformly high expression of *BCL6* within DLBCL, since *BCL6* transcript levels were found to be significantly lower in DLBCL than in non-malignant B-cells (Supplementary Fig. 1). Together, these data led us to hypothesize that *BCL6* may act in a 'hit-and-run' fashion and promote oncogenesis by transient overexpression during an early stage of haematopoietic differentiation or tumour evolution, and that its expression is no longer maintained or required in fully evolved tumour cells.

***BCL6* expression in human haematopoietic precursors.** To investigate the potential for *BCL6* to be acting at an early stage of haematopoietic differentiation, we performed gene expression profiling of 183 single-sorted human haematopoietic stem/progenitor cells (HSPCs) from bone marrow aspirates of two healthy adults (Supplementary Fig. 2). Single-cell profiling was used in order to allow evaluation of small populations of cells possessing unique gene expression phenotypes that may not be discernible from analysis of bulk populations. Using the beta-2-microglobulin (*B2M*) gene as a reference for successful RNA amplification and gene expression microarray analysis, we

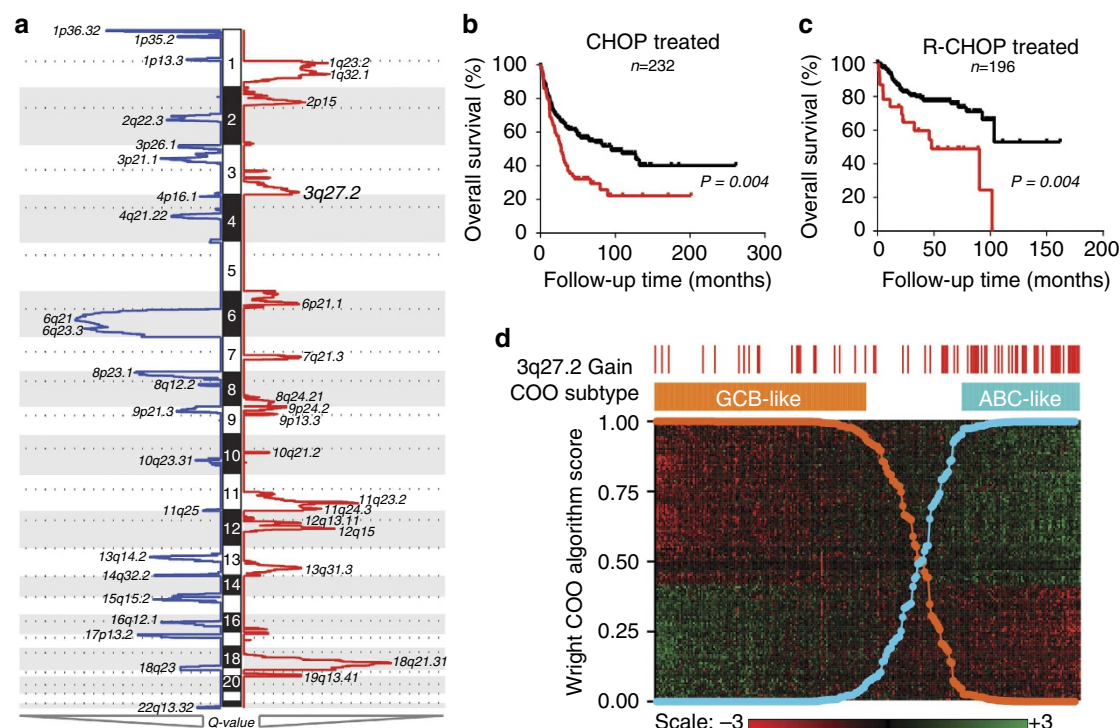


Figure 1 | High-resolution DNA copy number profiling of human DLBCL. (a) DNA copy number profiles from 609 primary DLBCL tumours were analysed for significant alterations using the GISTIC algorithm. This algorithm uses the magnitude and frequency of alterations at each position in the genome to assign a GISTIC Q value, with decreasing values indicating increasing significance. Significant peaks (GISTIC Q value <0.10) of DNA copy number loss (blue) and gain (red) are annotated with their genomic location. (b) In 232 patients treated with combination chemotherapy (CHOP) in the absence of Rituximab, presence of 3q27.2 gain (red) was associated with significantly worse overall survival than those with diploid copy number at this region (black). Log-rank P -value = 0.004. (c) Gain of 3q27.2 (red) remained to be associated with significantly worse overall survival compared with diploid 3q27.2 (black) in 196 patients treated with combination chemotherapy plus Rituximab (R-CHOP). Log-rank P -value = 0.001. (d) For 249 cases with matched gene expression profiling data, tumours were classified into GCB-like (orange) and ABC-like subtypes (blue) based upon the Wright 140 gene algorithm (heatmap shown). Gain of 3q27.2, shown by red tick marks for each case in which it was detected, was significantly over-represented in the ABC-like subtype compared with the GCB-like subtype (Fisher P value ≤ 0.001).

observed that *BCL6* transcript was detectable in 6.5% (6/92, donor 1) to 7.7% (7/91, donor 2) of single HSPCs (Fig. 3a). Notably, HSPCs expressing *BCL6* lacked significant expression of other markers of B-cell differentiation, including *PAX5*, *CD19* or *CD20* (*MS4A1*), among others. Nonetheless, gene set enrichment analysis (GSEA) found significant repression of *BCL6*-bound target genes²⁵ within the population of cells with expressing *BCL6* transcript compared with those cells not expressing *BCL6* (Fig. 3b). Thus, in a minor subset of adult human HSPCs, *BCL6* expression is associated with an early transcriptional program, consistent with similar observations in human cord blood, implicating this transcription factor in the commitment of specific progenitors to the lymphoid fate²⁶.

We therefore hypothesized that *BCL6* may contribute to lymphomagenesis at a stage of development before B-cells reach full maturity. Because *BCL6* shows highly conserved patterns of expression between humans and mice²⁷, we tested the hypothesis by generating a murine strain that transiently expressed *Bcl6* specifically within HSPCs by placing a floxed *Bcl6* cDNA with an internal ribosome entry site and enhanced green fluorescent protein (IRES-eGFP) marker under control of the promoter for the *Ly6A* locus encoding stem cell antigen-1 (*Sca1*; *Sca1-Bcl6*^{flxed}) (Fig. 3c; ref. 28). As expected, using flow cytometric analysis of the co-expressed GFP marker, we detected expression in hematopoietic stem cells (HSCs) and multipotential progenitors (MPP), with expression declining in common lymphoid progenitors (CLP) towards barely detectable expression in pre-pro-B cells and no detectable expression

in pro-B cells or later stages of B-cell development (Fig. 3d and Supplementary Fig. 3). Therefore, this transient expression of *Bcl6* during early haematopoietic development provided a means to evaluate the potential for *Bcl6* to contribute to lymphoma development via a 'hit-and-run' mechanism.

Transient *Bcl6* expression induces mature B-cell lymphoma.

Sca1-Bcl6^{flxed} mice are viable and develop normally, with a typical haematopoietic system early in post-gestational development and normal germinal centre development in response to a T-cell-dependent immunogen (Supplementary Fig. 4). However, by 4 weeks of age, increased numbers of HSCs, Lin-Sca1⁺ c-Kit⁺ (LSK) and lineage-restricted progenitors (Lin-CD48⁺ CD150⁺), and decreased numbers of common lymphoid progenitors (Lin-Sca1⁺ CD127⁺ c-Kit⁺) can be detected (Supplementary Fig. 5). In 8-week-old mice, we also noted changes in multiple lymphocyte compartments within the bone marrow, thymus, spleen and peripheral blood (Supplementary Fig. 6). In an ageing mouse colony, *Sca1-Bcl6*^{flxed} mice exhibit significantly shortened life span compared with wild-type (WT) littermates owing to the development of B-cell lymphomas in 50% (21/42) of mice (Fig. 4a). These lymphomas are manifested as expanded and confluent white pulp nodules composed of pleomorphic large B-cells resulting in splenomegaly (Fig. 4b,c). The lymphoma cells lack *Bcl6* expression but express hallmarks of B-cell identity, such as the *Pax5* transcription factor (Fig. 4d).

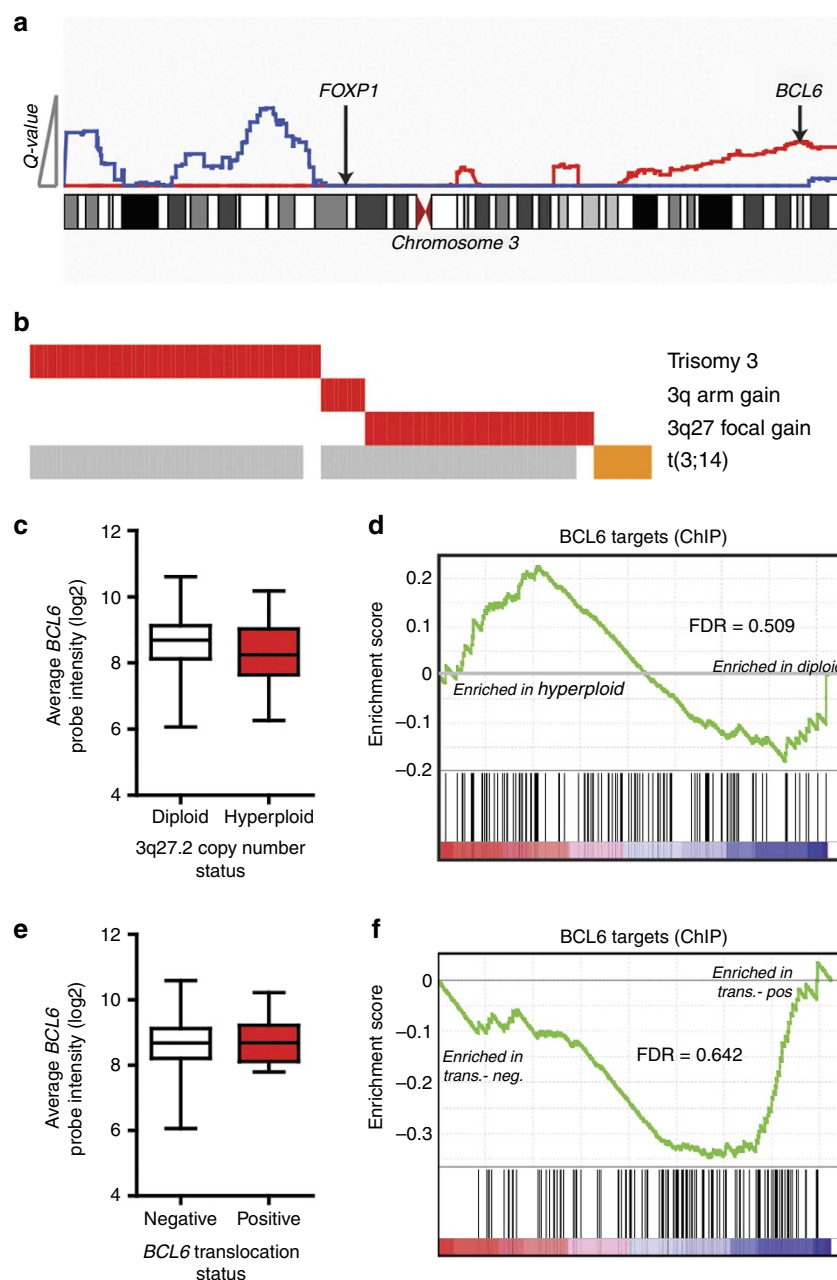


Figure 2 | 3q27.2 gain targets *BCL6* but does not alter its expression or target-gene repression. (a) GISTIC Q values are shown for DNA copy number loss (blue) and gain (red) on chromosome 3. The peak of 3q27.2 gain included the *BCL6* oncogene, but not the previously described target *FOXP1*. (b) Significance of 3q27.2 gain was contributed to by broad gains of chromosome 3 or the 3q arm in 76 tumours, as well as focal gains of 3q27 in 52 tumours. These gains were mutually exclusive to *BCL6* translocation in the 21 tumours for which matching DNA copy number and fluorescence *in situ* hybridization data were available. Grey bars represent data not available. (c) Increased DNA copy number of *BCL6* was not associated with increased transcript abundance compared with cases with no gain. Box plots represent the mean \pm the interquartile range with whiskers extending to the minimum and maximum value. (d) GSEA of *BCL6* target genes showed no significant repression within cases possessing *BCL6* DNA copy number gain (GSEA FDR = 0.509). (e) For the 58 tumours with matching *BCL6* translocation status and gene expression profiling data, *BCL6* transcript abundance was not increased in tumours with *BCL6* translocation compared with tumours without *BCL6* translocation. Box plots represent the mean \pm the interquartile range with whiskers extending to the minimum and maximum value. (f) Tumours with *BCL6* translocation (Trans. pos.) showed no significant repression of *BCL6* target genes by GSEA (GSEA FDR = 0.642) compared with tumours without *BCL6* translocation (Trans. neg.).

These results therefore provide the first indication that transient expression of the *Bcl6* oncogene in HSPCs can induce aggressive malignancies of mature B-cells.

***Sca1-Bcl6^{flox}* DLBCL tumours resemble post-GCB cells.** We next sought to evaluate the relationship of this model with the

trends observed in human DLBCL by assessing whether these malignancies resembled cells at a GCB or post-GCB (ABC/plasmablast) stage of differentiation. Using transcriptome analysis, we identified 750 significantly repressed and 720 significantly induced genes (*T*-test false discovery rate (FDR) < 0.25) in tumour-bearing spleens from *Sca1-Bcl6^{flox}* mice compared with spleens from WT mice, including increased expression of

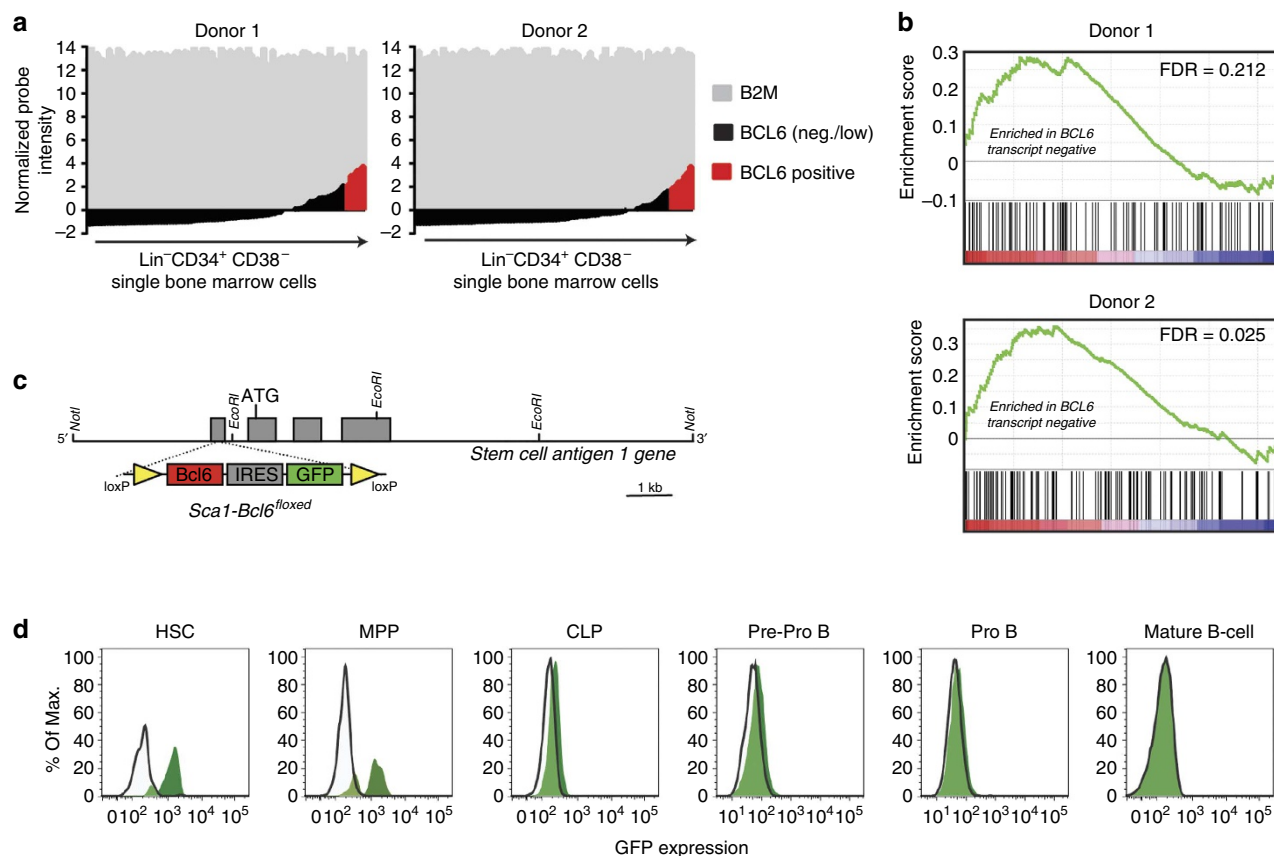


Figure 3 | Expression and activity of *BCL6* in human and murine HSPCs. (a) Gene expression profiles of single human HSPCs showing expression of the control gene *B2M* were investigated for expression of *BCL6*. Positive expression values defined as being 2 s.d.'s above the mean were observed in 11/183 single cells, with approximately equal proportions in each donor. (b) GSEA of *BCL6* target genes in *BCL6* transcript-positive cells compared with *BCL6* transcript-negative cells in each donor showed an enrichment of target-gene expression in *BCL6* transcript-negative cells (GSEA FDRs = 0.212 and 0.025 for Donor 1 and 2, respectively). This corresponds to repression of target genes in *BCL6* transcript-positive cells. (c) Transient *Bcl6* expression within HSPCs was achieved by placing a floxed (yellow loxP sites) *Bcl6* cDNA with IRES-GFP reporter under control of the promoter for the HSPC-specific gene, stem cell antigen-1 (*Sca1*). (d) Tracking of the GFP marker for *Bcl6* transgene expression during haematopoietic development shows expression is restricted to HSPCs and not in Pro-B or mature B-cells. Images are representative of four independent experiments. For gating schema, see Supplementary Fig. 3.

multiple genes with roles in oncogenesis (Fig. 5a and Supplementary Data 1). However, *BCL6* target genes were not significantly repressed within these tumours (GSEA FDR = 1.000; Fig. 5b). This is consistent with our findings from human DLBCL tumours, and further supports a 'hit-and-run' role for *Bcl6* in generating these aggressive B-cell malignancies. Human DLBCL tumours can be reliably classified into GCB-like or ABC-like subtypes by gene expression profiling¹, and this can be achieved in murine models because of recent mapping of the transcriptional signatures of normal murine B-cell development^{29,30}. Using the broad transcriptional signature of tumours from *Sca1-Bcl6*^{flxed} mice compared with signatures of normal stages of murine B-cell development, we found these tumours to most significantly align with the post-germinal centre ABC/plasmablast stage of differentiation (hypergeometric enrichment *P* value = 0.028, FDR = 0.017; Fig. 5c). These changes included increased transcript abundance of the post-germinal centre transcription factors *Irf4*, *Prdm1* and *Xbp1* (Fig. 5d). In addition, immunohistochemical staining of tumours from *Sca1-Bcl6*^{flxed} mice showed no staining for the GCB marker peanut agglutinin (PNA), but strong staining for *Irf4* and the ABC-like DLBCL marker FoxP1 (Fig. 5e). These data therefore demonstrate that transient expression of the *Bcl6* oncogene within HSPCs of *Sca1-Bcl6*^{flxed} mice is capable of inducing

aggressive B-cell tumours that align with a differentiation stage comparable to human ABC-like DLBCL.

Evidence for HSPCs as lymphoma-initiating cells. To exclude the potential contribution to lymphomagenesis of persistent ectopic *Bcl6* expression in the mature B-cell compartment, we crossed the *Sca1-Bcl6*^{flxed} mice with an mb1-Cre mouse strain. The resulting strain, *Sca1-Bcl6*^Δ, maintains expression of *Bcl6* under the *Sca1* promoter in HSPCs, but deletes the exogenous floxed *Bcl6* cDNA upon B-lineage commitment via Cre-recombinase driven by the promoter from mb1 locus encoding the immunoglobulin-associated alpha-chain *Cd79a* (Fig. 6a). To validate the efficient deletion of the exogenous floxed *Bcl6* cDNA, we sorted B220⁺ cells from bone marrow of young *Sca1-Bcl6*^Δ mice and cultured under conditions to allow the isolation and expansion of a pure population of B220⁺c-Kit⁺ pro-B cells. Southern blot analysis of DNA from these cells confirmed uniform and efficient deletion of the exogenous floxed *Bcl6* cDNA at the pro-B stage, and therefore all subsequent stages, of B-cell differentiation (Fig. 6b and Supplementary Fig. 7).

Importantly, *Sca1-Bcl6*^Δ mice recapitulate the phenotype observed in *Sca1-Bcl6*^{flxed} mice. These mice have a shortened survival compared with WT littermates (Fig. 6c) because of

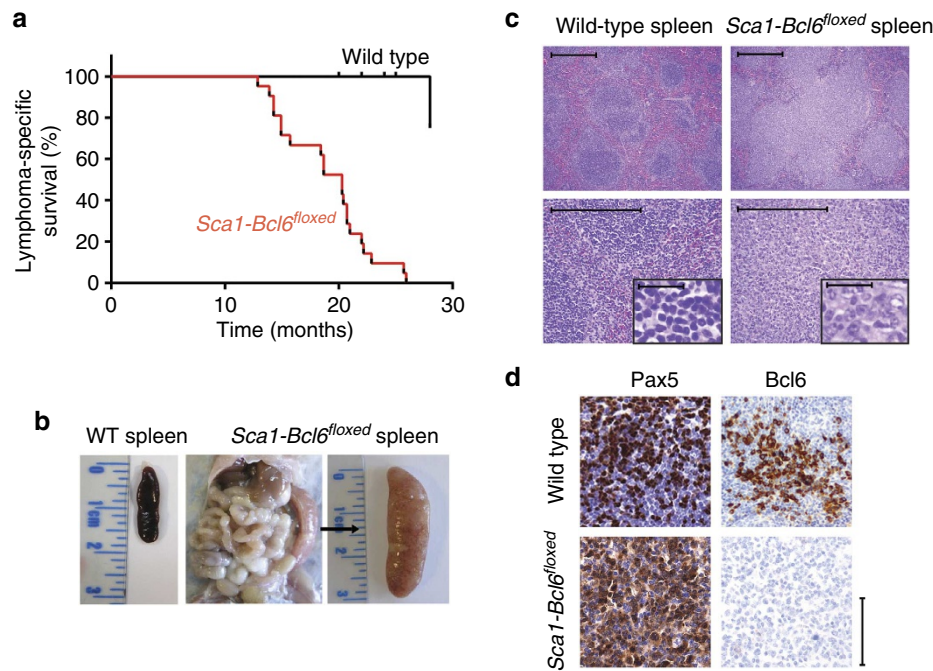


Figure 4 | Expression of the *Bcl6* oncogene in haematopoietic progenitor cells (HSPCs) causes aggressive malignancy of mature B-cells that lack *Bcl6* protein expression. (a) Lymphoma-specific survival of *Sca1-Bcl6*^{flxed} mice (red, *n* = 21), showing a significantly (log-rank *P* value < 0.001) shortened life span compared with WT mice (black, *n* = 20) as a result of mature B-cell malignancies. (b) Example of splenomegaly observed in 50% (21/42) of *Sca1-Bcl6*^{flxed} mice. A spleen from a WT mouse is shown for reference. (c) Haematoxylin and eosin staining of WT spleens and tumour-bearing spleens from *Sca1-Bcl6*^{flxed} mice shows loss of normal architecture resulting from effacement with cells morphologically resembling lymphocytes (above = × 10, below = × 40 and inset = × 400). Images are representative of ≥ 3 replicates. Scale bar represents 100 μm for large panels, 50 μm for inset. (d) Immunohistochemistry shows that lymphocytes from *Sca1-Bcl6*^{flxed} tumours bear markers of B-cell identity (Pax5), but lack protein expression of *Bcl6*. WT spleens obtained from immunized mice. Scale bar represents 200 μm for all panels.

aggressive B-cell malignancy in 56.50% (13/24) of mice, manifesting as splenomegaly resulting from complete effacement of normal architecture by diffuse B-cell infiltration (Fig. 6d,e). Malignant B-cells are primarily immunoglobulin M (IgM⁺) but show evidence of heavy-chain class-switch in a subset of tumours (Supplementary Fig. 8). These mice also showed infiltration of malignant cells into the liver and bone marrow, resulting in disruption of normal architecture (Fig. 6e). Tumours showed increased clonality of immunoglobulin rearrangements (Supplementary Fig. 9), and significant similarity to *Sca1-Bcl6*^{flxed} tumours at the transcriptional level (Supplementary Fig. 10). In line with *Sca1-Bcl6*^{flxed} tumours, *Sca1-Bcl6*^Δ tumours also expressed markers of B-cell identity and a post-germinal centre stage of differentiation (Supplementary Fig. 10). To identify the tumour repopulating cells for *Sca1-Bcl6*^Δ lymphomas, we purified LSK and B220⁺ cells and transplanted them into sublethally irradiated syngeneic recipient mice. Each of the mice transplanted with LSK cells developed a DLBCL that was phenotypically identical to the primary disease. In contrast, the B220⁺ cells were incapable of inducing lymphoma in secondary recipients, even when injected in a 10- or 100-fold higher number than the LSK cells (Supplementary Table 2), despite these cells being able to transplant disease in other models³¹. This indicates that *Bcl6*-induced DLBCL in this model is propagated by transformed HSPC cells but not mature tumour cells, and confirm that activity of the *Bcl6* oncogene restricted to HSPCs can induce malignancies in mice that are of a post-germinal centre stage of differentiation.

p53 loss in *Sca1-Bcl6*^{flxed} mice does not promote lymphoma. Prior studies have shown that *Bcl6* acts in myeloid leukaemia

stem cells and normal B-cell development by inactivation of p53 and subsequent sensing of DNA damage^{11,12}. We therefore evaluated whether the inactivation of p53 and the accumulation of secondary genetic alterations have a role in this model by crossing *Sca1-Bcl6*^{flxed} mice with heterozygous (p53^{+/-}) or homozygous (p53^{-/-}) p53 knockout mice. This showed that decrease or loss of p53 did not facilitate B-cell lymphoma development, but instead resulted in myeloid neoplasia (Supplementary Fig. 11). B-cell lymphoma development in *Sca1-Bcl6*^{flxed} mice therefore may not proceed via suppression of p53 and the accumulation of secondary genetic lesions as observed in myeloid malignancies. Exome sequencing of *Sca1-Bcl6*^{flxed} tumours revealed the accumulation of many somatic variants, but none that were recurrent across tumours or that had been implicated in lymphomagenesis. We also noted an absence of DNA copy number abnormalities that are associated with p53 deregulation in lymphoma³² (Supplementary Fig. 12 and Supplementary Data 2). Together these data show that p53 dysfunction in combination with *Bcl6* promotes myeloid malignancy, as previously described¹¹.

Epigenetic changes associated with transient *Bcl6* expression. *Bcl6* mediates suppression of target genes via recruitment of factors that epigenetically modify chromatin. We hypothesized that this may elicit changes in DNA methylation, a mark that is capable of acting in gene-silencing memory³³, and therefore investigated whether this may be a potential mechanism for *Bcl6*-mediated ‘hit-and-run’ oncogenesis. Using genome-wide DNA methylation profiling by reduced representation bisulfite sequencing of populations of HSPCs and mature B-cells from WT and *Sca1-Bcl6*^Δ mice, we identified broad epigenetic changes associated with

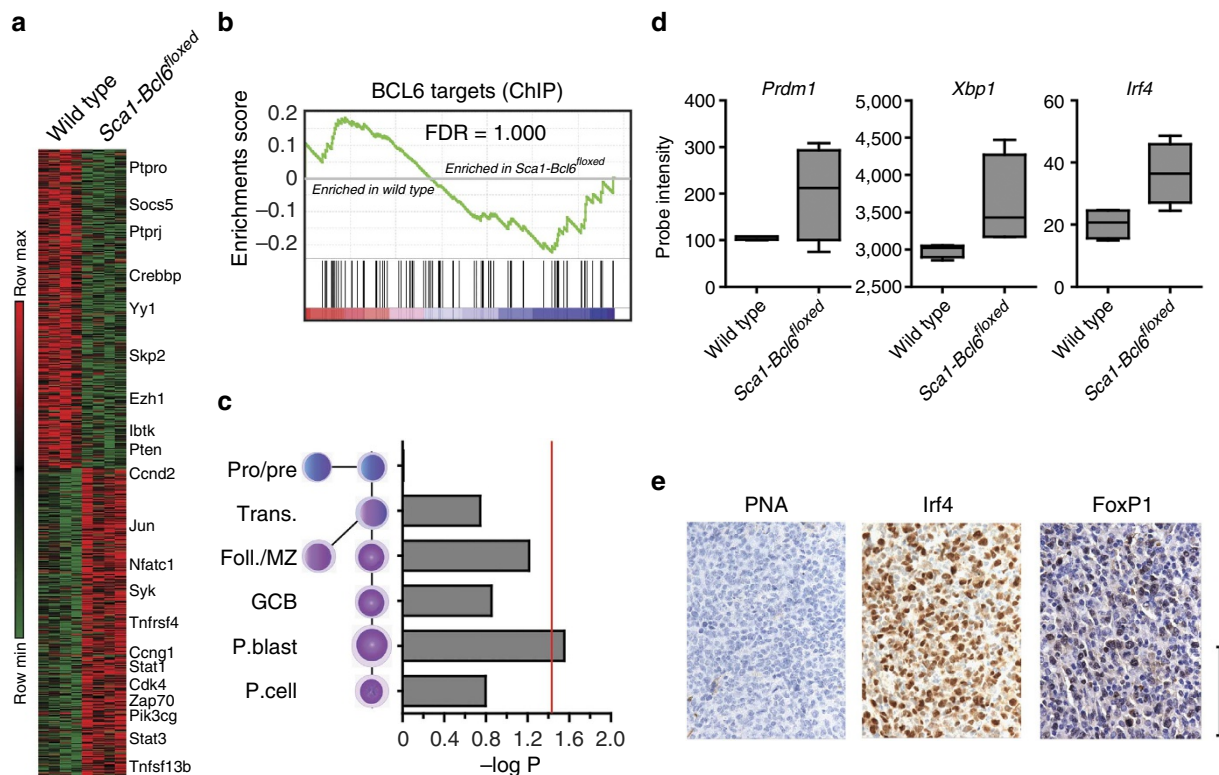


Figure 5 | Tumours from *Sca1-Bcl6^{flox}* mice resemble post-GCB cells. (a) Differential gene expression analysis of tumour-bearing spleens of four *Sca1-Bcl6^{flox}* mice compared with spleens from four WT mice show significant differences. These differences include genes that are involved in B-cell signalling and cell cycle regulation. (b) GSEA identified no significant repression or derepression of *Bcl6* target genes in *Sca1-Bcl6^{flox}* tumour-bearing spleens compared with spleens from WT mice (GSEA FDR=1.000). This is in line with what is observed in human DLBCL that possess amplification of the *BCL6* coding region. (c) Analysis of differentially expressed genes in *Sca1-Bcl6^{flox}* tumour-bearing spleens with relation to gene expression signatures of normal murine B-cell differentiation including Pro/pre-B, transitional (Trans.) B-cells, follicular and marginal zone (Foll./MZ) B-cells, GCB cells, plasmablasts (P.blast) and plasma cells (P. cell). This shows significant enrichment of the normal plasmablast signature (hypergeometric enrichment P value = 0.028, FDR = 0.17). Red line represents a hypergeometric enrichment P value of 0.05. (d) Tumours from *Sca1-Bcl6^{flox}* mice show increased expression of transcription factors that are associated with post-germinal centre stages of B-cell differentiation. Box plots represent the mean \pm the interquartile range with whiskers extending to the minimum and maximum value. (e) Immunohistochemical staining shows negative expression of the germinal centre marker peanut agglutinin (PNA), but positive staining for the post-germinal centre transcription factor *Irf4*, and the ABC-like DLBCL marker FoxP1. Images are representative of ≥ 3 replicates. All panels are $\times 60$, scale bar, 100 μ m.

the expression of *Bcl6* in HSPCs (Fig. 7a and Supplementary Data 3). Importantly, a significant subset of these changes were found to be maintained from HSPCs to mature B-cells in *Sca1-Bcl6^{flox}* mice, resulting in these populations being epigenetically more similar to each other than to their comparative population from WT mice (Fig. 7a,b). Genomic regions found to have significant changes in DNA methylation that contained a significantly higher representation of *Bcl6* DNA-binding motifs compared with those regions that showed no change in DNA methylation (Fig. 7c), but were not significantly enriched for genes found to be bound by *Bcl6* using chromatin immunoprecipitation-sequencing (ChIP-seq) analysis of mature human B-cells²⁵ (hypergeometric enrichment FDR=0.990). This trend was particularly notable in genes found to be hypermethylated in *Sca1-Bcl6^{flox}* HSPCs and mature B-cells compared with their WT counterparts. Intriguingly, concordantly hypermethylated genes in HSPCs and mature B-cells from *Sca1-Bcl6^{flox}* mice were significantly enriched for gene sets associated with murine and human stem cells and poor outcome in human DLBCL (Fig. 7d and Supplementary Table 3). Although this analysis was not performed on post-GCB tumour B-cells, we suggest that these results implicate epigenetic alterations that are imparted during transient *Bcl6* expression and maintained thereafter as a mechanism for *Bcl6* 'hit-and-run' oncogenesis.

Discussion

It is well established that cancer arises via the stepwise acquisition of somatic alterations that transition clones via one or more premalignant states to a malignant state³⁴. But deconvolution of the stepwise events taking place during tumour cell evolution is difficult because of the many genetic alterations that become clonally dominant by the time of their interrogation within the clinically manifested tumour, and the multitude of avenues by which any given tumour can evolve. However, research within the cancer stem cell field has led to a growing appreciation for the potential of oncogenic events to be acquired by tumour cell precursors that exist at an earlier differentiation state than the evolved tumour clone^{16,35}. Although several prior studies have implicated aberrations within HSPCs as important for driving neoplasms of mature B-cells including chronic lymphocytic leukemia¹⁷ and follicular lymphoma^{13,36}, there has not yet been any suggestion that a similar mechanism may be relevant for DLBCL.

By high-resolution genomic analysis of a large number of human DLBCL tumours, we identified DNA copy number gain of 3q27.2 as being important for DLBCL disease biology because of its significant association with adverse outcome and the aggressive ABC-like disease subtype. Similar to many SCNAs, the minimal region of significant copy number gain on 3q27.2

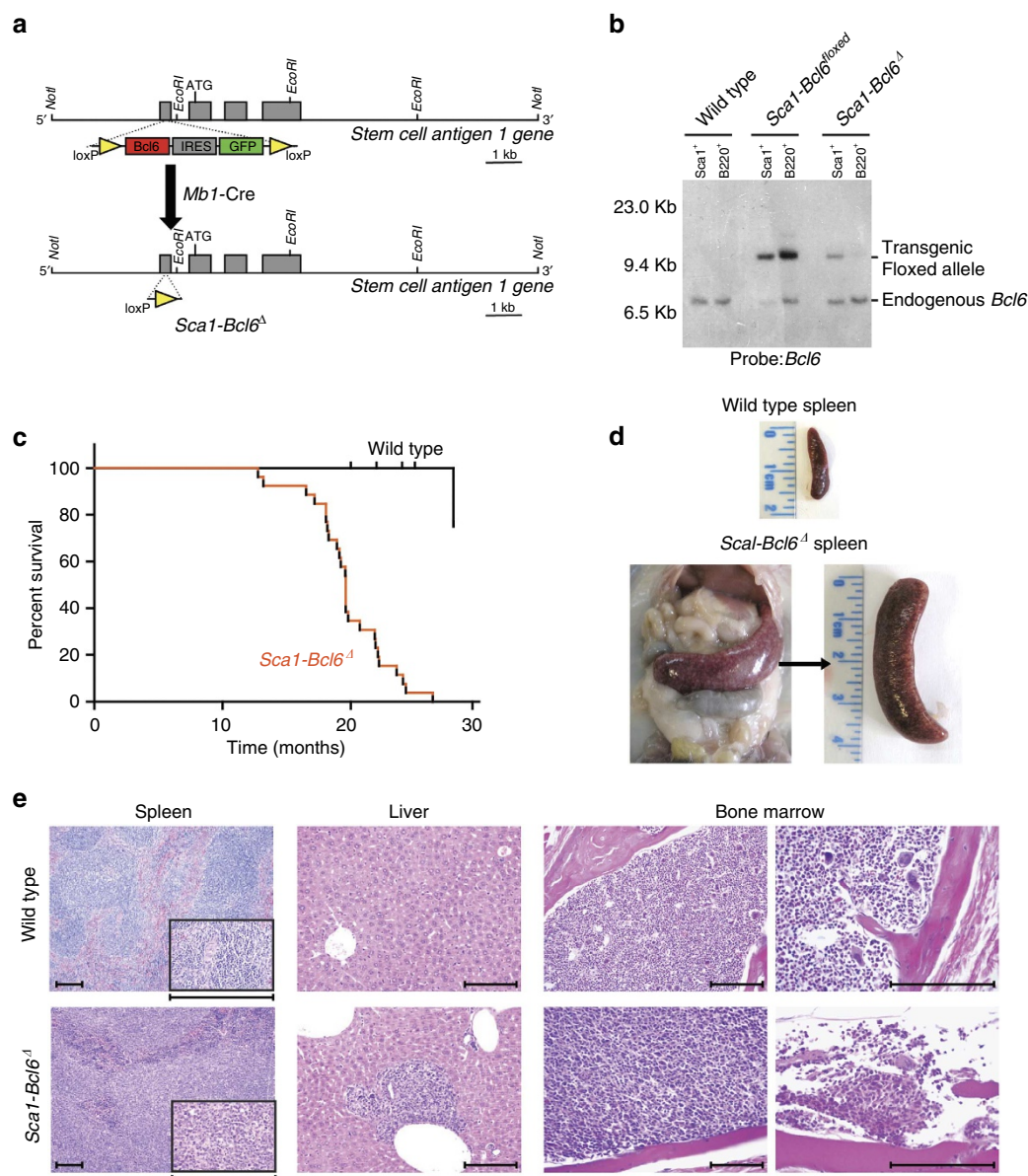


Figure 6 | Cre-mediated deletion of the exogenous *Bcl6* allele in precursor B-cells does not alter formation of mature B-cell malignancies.

(a) Diagrammatic representation of the *Sca1-Bcl6^Δ* mice, showing expression of the transgenic *Bcl6* allele within HSPCs under control of the *Sca1* promoter, followed by Cre-mediated deletion at an early Pro-B cell stage upon *Mb1* expression. (b) Southern blot analysis confirms absence of the transgenic *Bcl6* allele within mature (B220⁺) B-cells of *Sca1-Bcl6^Δ* mice. Image is representative of three replicate experiments. (c) Lymphoma-specific survival of *Sca1-Bcl6^Δ* mice (*n* = 13) demonstrates a significantly (log-rank *P* value < 0.001) shorter life span compared with WT mice (*n* = 20). (d) Example of splenomegaly observed in *Sca1-Bcl6^Δ* mice, with spleen from a WT mouse is shown for reference. Images are representative of 13 mice. (e) Effacement of spleen ($\times 100$, inset $\times 400$) by malignant B-cells and infiltrates in the liver ($\times 200$) and bone marrow (left $\times 200$, right $\times 400$) result in loss of normal architecture. Images representative are of 13 mice. Scale bar, 200 μm.

contained multiple genes. However, the propensity for the *BCL6* oncogene to be targeted by other genetic alterations in DLBCL, such as point mutations and translocation that deregulate its expression^{24,6,37}, and the mutual exclusivity of *BCL6* translocation with its DNA copy number gain, strongly suggested that *BCL6* was a target of this alteration. Integrative analysis of DNA copy number and transcriptome data further suggested that *BCL6* may act in a ‘hit-and-run’ fashion, wherein its transient overexpression is promoted by genetic alteration but is not maintained in the evolved tumour cell population.

The *BCL6* gene encodes a POZ/zinc-finger transcriptional repressor that regulates gene expression in a manner that is independent of the location of its binding site, via interaction with

co-repressors that recruit histone deacetylases and induce epigenetic remodelling and heterochromatin formation³⁸. The best characterized role of *BCL6* is within normal B-cell activation and germinal centre formation, but its expression is not limited to the B-cell compartment and contributes to the normal function of other cellular populations, including multiple T-cell subsets and macrophages^{22,39–42}. Recently, a role for *BCL6* has also been described within progenitor populations during normal haematopoiesis and in the function of cancer stem cells in myeloid leukaemia^{11,12,26}. Laurenti *et al.*²⁶ identified *BCL6* transcript expression in human cord blood HSPCs and found that extinguishing this expression resulted in decreased numbers of mature B-cells, suggesting that *Bcl6* expression in

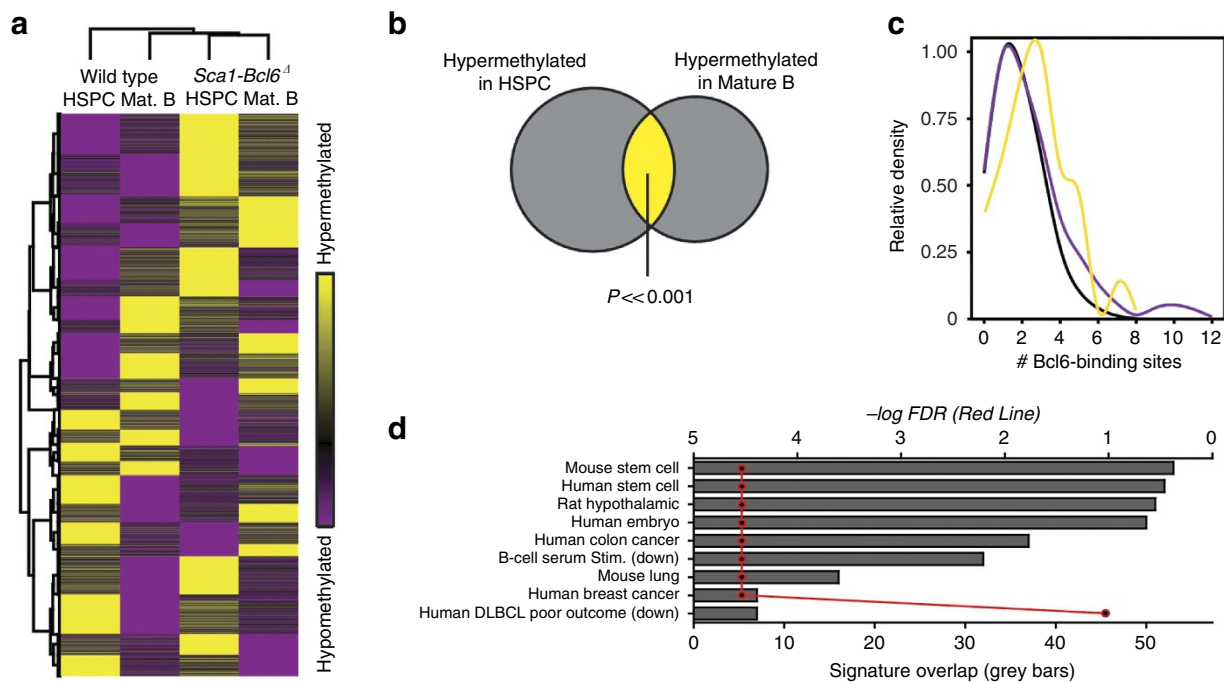


Figure 7 | *Bcl6* expression in HSPCs induced broad epigenetic changes. (a) Unsupervised hierarchical clustering of methylation ratio data from 11,258 promoter regions revealed that HSPCs and mature B-cells (Mat. B) from *Sca1-Bcl6*^Δ mice are epigenetically more similar to each other than to their respective counterparts from WT mice, again suggesting that *Bcl6* acts via an epigenetic mechanism that persists from HSPCs to mature B-cells. Each condition represents a pool of biological replicates from 6 to 9 mice. (b) HSPCs and mature B-cells from *Sca1-Bcl6*^Δ mice show significant hypermethylation of a large number of genes compared with the same subsets from WT mice (Supplementary Data 3). These included a significant overlap of 470 genes, suggesting that *Bcl6* creates an epigenetic signature in the HSPCs that is maintained through differentiation and can be found in the mature B-cell compartment. (c) Kernel density plot of the number of BCL6 DNA-binding sequence motifs identified in genomic regions with significant hypermethylation (yellow) or hypomethylation (purple) in both HSPCs and mature B-cells from *Sca1-Bcl6*^Δ compared with WT mice (P value < 0.05) and in regions with no change in methylation (black) between *Sca1-Bcl6*^Δ and WT mice ($P > 0.95$). Hypermethylated regions showed a significant (P value < 0.001) increase in the abundance of BCL6-binding motifs compared with regions with no change in methylation. Hypomethylated regions also showed a significant, but less dramatic, increase in abundance of BCL6-binding motifs (P value < 0.001). P values calculated by Mann-Whitney U -test. (d) Hypergeometric GSEA of the list of genes that were hypermethylated in both HSPCs and mature B-cells of *Sca1-Bcl6*^Δ mice showed significant enrichment (hypergeometric enrichment FDR < 0.25) of multiple gene sets, including those associated with murine and human stem cells, and with poor outcome in DLBCL. The number of overlapping genes between those with conserved hypermethylation and those present in listed genes sets are shown by grey bars (bottom x axis), with the corresponding FDR for the hypergeometric enrichment shown by the red line (top x axis).

HSPCs has a critical role in early B-cell development. Our observation of *BCL6* expression in a subset of adult human bone marrow HSPCs, and the associated coordinate repression of *BCL6* target genes within these cells, adds to growing evidence for a role of *BCL6* in normal early human haematopoiesis. It is therefore plausible that genetic deregulation of *BCL6* within these cells by DNA copy number gain or translocation could potentially contribute to the pathogenesis of diseases such as leukaemia and lymphoma. The oncogenic function of *BCL6* may also potentially act in the germinal centre, with repression occurring thereafter as a result of processes that occur during normal B-cell differentiation. However, transgenic mice expressing *Bcl6* in mature B-cells under the control of the immunoglobulin promoter required repeated immunization in order to induce lymphoma⁴³. In contrast, immunization was not required to induce lymphoma in *Sca1-Bcl6*^{flxed} or *Sca1-Bcl6*^Δ mice that expressed *Bcl6* transiently within HSPCs, suggesting that the lymphomagenic potential of *Bcl6* may be stronger within this compartment.

As patterns of *BCL6* expression are tightly conserved between humans and mice²⁷, we modelled this hypothesis by expression of *Bcl6* transiently within murine HSPCs. The lymphomas that developed in these mice were histologically similar to human DLBCL and transcriptionally similar to the differentiation stage

of human ABC-like tumours in which *BCL6* SCNAs were identified. Also in line with our observations in human ABC-like DLBCL, the murine lymphomas did not show overexpression of *Bcl6* or coordinate target-gene repression, suggesting that *Bcl6* was acting in a 'hit-and-run' fashion. This was further confirmed by Cre-mediated deletion of the exogenous *Bcl6* allele upon B-cell maturity, which did not alter the development or phenotype of these tumours. Because *BCL6* can alter the activity of the p53 tumour suppressor gene⁴⁴, and this is critical for leukaemia stem cell survival in chronic myeloid leukaemia¹², we investigated whether the lymphomagenic potential of transient *Bcl6* expression was via repression of p53 and the accumulation of secondary genetic alterations. Crossing of *Sca1-Bcl6*^{flxed} mice with p53^{+/-} and p53^{-/-} mice did not accelerate the development of DLBCL, but instead promoted myeloid malignancies. These myeloid malignancies may have masked the development of lymphoid malignancies that have longer latency periods, but shows that combined deregulation of *Bcl6* and p53 has a relatively more profound role in myeloid compared with lymphoid tumorigenesis. Furthermore, lymphomas from *Sca1-Bcl6*^{flxed} mice did not show patterns of DNA copy number change or somatic mutation that are associated with p53 malfunction in lymphoma³², indicating that *Bcl6* may be acting 'hit-and-run' oncogenesis within this model in a manner that is

not promoted by p53 dysfunction. Although the exact mechanism by which transient *Bcl6* expression promotes oncogenesis remains to be defined, we found some evidence that suggests that *Bcl6* may function by inducing epigenetic changes that were conserved from HSPCs to mature B-cells in *Sca1-Bcl6^Δ* mice. In addition, the reduced polyclonality of B-cell lymphomas from these mice suggested that there may be additional genetic, epigenetic or microenvironmental factors following V(D)J (Variable, Diverse and Joining gene segments) recombination that confer a growth advantage to some clones.

Our observations in the mouse model described here are potentially relevant to human disease, providing some evidence for 'hit-and-run' oncogenesis in ABC-like DLBCLs that could be linked to *BCL6*. Several lines of evidence support such a linkage. First, genetic aberrations targeting *BCL6* in human DLBCL do not result in its significant overexpression or coordinate repression of its target genes. Second, we observed that genes with conserved *Bcl6*-induced hypermethylation between HSPC and mature B-cells of *Sca1-Bcl6^Δ* mice are significantly enriched for markers distinguishing human DLBCL patients with fatal/refractory disease from those that are cured. Third, correlation between DLBCL subtype and immunoglobulin heavy-chain isotype highlights an important paradox between the differentiation stage and the isotype of the B-cell receptor. Specifically, despite similar levels of activation-induced cytidine deaminase (AID) expression¹⁰, ABC-like DLBCL do not exhibit evidence of productive heavy-chain class-switching^{45,46} or ongoing somatic mutation⁴⁷. This suggests that the mature ABC phenotype of ABC-like DLBCL is disconnected from their less mature immunoglobulin genotypes. Finally, in patients presenting with relapsed/refractory disease, DLBCL subtypes exhibit differential sensitivity to salvage chemotherapy regimens as part of autologous stem and progenitor cell transplantation studies⁴⁸, raising the hypothesis that differences in therapy might modulate *BCL6* expression through epigenetic mechanisms. Although our model of 'hit-and-run' oncogenesis is not compatible with those genes that induce 'oncogene-addiction' (for example, *MYC*⁴⁹), it may be compatible with other genes that are able to induce long-lasting epigenetic changes. Whether a subset of human ABC-like DLBCL tumours have their roots in genetic aberrations arising in early HSPCs or in a more mature stem-like lymphoid subpopulation requires further study. Definitive staging of somatic genetic lesions is not obvious because tumours can exhibit phenotypes of one stage of development but contain translocations from prior stages. For example, while *BCL6*, *MYC*, *BCL2* and *BCL1* translocations are all found in mature B-cell lymphomas, these lesions are distinguished by hallmarks such as immunoglobulin recombination signal sequences and junctional additions at translocation break points, suggesting their distinct derivation from early or late events during B-cell development^{44,50}. Separately, evidence for lineage plasticity of mature lymphomas^{17,36} complicates inferences of cell of origin that are based on either gene expression profiles or genotypes alone. It is therefore unclear as to the specific stage of haematopoietic or B-cell differentiation before evolved DLBCL that *BCL6* acts, and the hierarchy of genetic events contributing to this disease will only be definitively defined by isolating human haematopoietic and tumour cell precursors from patients and identifying the minimal set of genetic lesions they harbour.

Based upon our observations, we propose a model wherein an oncogene may act in a 'hit-and-run' fashion within early tumour cell precursors and is no longer required in the evolved tumour cell progeny. Evolved tumour cells may in turn become reliant on alternate survival pathways that are not present within their precursors. We propose that in human ABC-like DLBCL, genetic alterations of *BCL6* may act in a 'hit-and-run' fashion in early

precursors, while evolved tumour cells develop reliance on alternative oncogenic mechanisms such as nuclear-factor κB and B-cell receptor signalling pathways^{51–52}. This may provide some explanation for the lower sensitivity of mature ABC-like DLBCL cell-lines to *BCL6* inhibition⁵³, despite the high prevalence of *BCL6* gene alterations, and the failure of some modern targeted therapies to clear tumour stem cells, despite being effective agents against evolved tumour cells. As a consequence, targeted treatment strategies may need to be altered to accommodate combinations of agents that target oncogenic pathways that are active at both the early and late stages of tumour development. Our findings therefore have important implications for understanding and therapeutically targeting tumour cells.

Methods

Integrative analysis of human DLBCL and normal B-cells. All human data was obtained from public databases and associated with informed consent obtained as part of the original source studies. DNA copy number data were obtained from 609 primary DLBCL tumour specimens^{23,32,54–56}, and were analysed by GISTIC2 (ref. 57). This represented all publicly available high resolution (> 244,000 markers) at the time this study was undertaken. Survival annotations were available for 232 CHOP-treated patients^{23,32} and 196 R-CHOP-treated patients^{32,54}, as described previously. These groups of patients were analysed separately because of the improved outcome of patients treated with Rituximab. *BCL6* translocation status determined by fluorescence *in situ* hybridization in 58 tumours with matched gene expression microarray data²⁴. Raw.cel files from Affymetrix U133 plus 2.0 gene expression microarray data of 163 tumours with matched DNA copy number data and/or *BCL6* translocation status^{23,24,32}, and for normal B-cell subsets and DLBCL tumours⁵⁸, were normalized by robust multi-array average (RMA) using the *ExpressionFileCreator* module of GenePattern⁵⁹, and batch corrected using ComBat⁶⁰. COO subtype was classified using the Wright algorithm of 140 genes⁶¹. These subtypes aligned with prior classification²³ for 125/163 cases, with the remaining discordances being transition between GCB and unclassified or ABC and unclassified, but not GCB and ABC. As a sanity check, COO was found to significantly stratify survival (log-rank *P* value < 0.001; Supplementary Fig. 13). For *BCL6* expression, the probe intensities of five probes specific for *BCL6* were averaged (203140_at, 215990_s_at, 228758_at, 236439_at and 239249_at). Comparison of *BCL6* expression between was performed using a two-sided *t*-test. GSEA was performed for *Bcl6* target genes using a previously described set of ChIP-validated target genes²⁵ and GSEA-P software⁶².

Single-cell gene expression profiling of human HSPCs. Bone marrow from two healthy donors (1 male and 1 female) was obtained from AllCells, LLC (Emeryville, CA, USA) and sorted on a FACS ARIA II instrument as *PI⁻*, *Lin⁻*, *CD34⁺* and *CD38⁻*. Single cells were sorted into Terasaki plates containing alternating rows of wells containing media or Miltenyi SuperAmp lysis buffer for a total yield of 96 single cells in lysate per donor; wells containing media were visualized under a microscope to provide visual confirmation that single cells were sorted into each well (Supplementary Fig. 2). For all four donors, bulk population samples were further sorted into Terasaki plates in additional groups (no further sort, HSC (CD90⁺ and CD45RA⁻), MPP (CD90⁻ and CD45RA⁻) and L-MPP (CD90⁻ and CD45RA⁺)), containing 200 – 10,000 cells. All antibodies were obtained from BD Biosciences. The lysates were shipped to Miltenyi Biotec (Auburn, CA, USA) and processed using their SuperAmp microarray service, where they amplified the lysates using their SuperAmp technology and hybridized probes made from amplified material onto SurePrint G3 Human Gene Expression 8 × 60K Microarrays (Agilent). Raw data were quantile normalized in R (Bioconductor pre-processCore library), and replicate microarray probes (representing the same gene) were log2 transformed and combined as the geometric mean. Single cells were classified as expressing *BCL6* if their intensity value was 2 s.d.'s above the mean for that donor.

Generation of *Bcl6* transgenic mouse strains. All animal work has been conducted according to relevant national and international guidelines and it has been approved by the Bioethics Committee of University of Salamanca and by the Bioethics Subcommittee of Consejo Superior de Investigaciones Científicas (CSIC). The *Bcl6*-floxed vector was generated by inserting the mouse *Bcl6*-IRES-eGFP cassette flanked by loxP sites into the *Clal* site of the pLy6 vector. The transgene fragment was excised from its vector by restriction digestion with *NotI*, purified and injected (2 ng ml⁻¹) into CBA × C57BL/6J-fertilized eggs. Transgenic mice were identified by Southern blot analysis of tail snip DNA after *EcoRI* digestion, using *Bcl6* cDNA to detect the transgene. Two independent transgenic lines were generated and analysed. *Sca1-Bcl6^{flxed}* mice were bred to *mb1-Cre* (*Cd79a^{tm1(Cre)}Rethy*) mice to generate *Sca1-Bcl6^Δ* mice. Upon signs of disease, mice were killed and subjected to standard necropsy procedures. All major organs

were examined under the dissecting microscope. Tissue samples were taken from homogenous portions of the resected organ and fixed immediately after excision. Differences in Kaplan–Meier survival plots of transgenic and WT mice were analysed using the log-rank (Mantel–Cox) test. To test the rearrangement in *Sca1-Bcl6^d* mice, different samples were analysed by Southern blot analysis after *EcoRI* digestion and using *Bcl6* cDNA as probe. PCR was also used for confirmation, with the following primers: ClaI-F2, 5'-TATAATCTGGCTTGATC AGG-3' and ClaI-R2, 5'-CTGAGGAATTCATGTCTGCC-3'.

Generation of *Bcl6*-floxed *p53*^{+/-} and *Bcl6*-floxed *p53*^{+/-} mice. The heterozygous *p53*^{+/-} mice⁶³ have been described previously. Heterozygous *p53*^{+/-} mice were bred to *Bcl6*-floxed mice to generate compound heterozygotes. F1 animals were crossed to obtain null *p53*^{-/-} mice hemizygous for *Sca1-Bcl6^{flox}* mice. Tumour phenotype was assessed in the first generation of *p53* heterozygous and homozygous mice.

Flow cytometry. Nucleated cells were obtained from total mouse bone marrow (flushing from the long bones), peripheral blood, thymus or spleen. In order to prepare cells for flow cytometry, contaminating red blood cells were lysed with red cell lysis buffer lysis buffer and the remaining cells were then washed in PBS with 1% fetal calf serum. After staining, all cells were washed once in PBS with 1% FCS containing 2 mg ml⁻¹ propidium iodide to allow dead cells to be excluded from both analyses and sorting procedures. The samples and the data were acquired in an AccuriC6 Flow Cytometer and analysed using FlowJo software. Specific fluorescence of FITC (fluorescein isothiocyanate), PE (phycoerythrin), propidium iodide and APC (allophycocyanin) excited at 488 nm (0.4 W) and 633 nm (30 mW), respectively, as well as known forward and orthogonal light-scattering properties of mouse cells were used to establish gates. Nonspecific antibody binding was suppressed by preincubation of cells with CD16/CD32 Fc-block solution (BD Biosciences). For each analysis, a total of at least 50,000 viable (PI-) cells were assessed.

The following antibodies were used for flow cytometry: anti-B220 (RA3-6B2), CD3e (145-2C11), CD4 (RM4-5, 1:500), CD8a (53-6.7, 1:500), CD11b/Mac1 (M1/70, 1:200), CD19 (1D3), CD49b (DX5), CD117/c-Kit (2B8, 1:200), CD127/IL-7Rα (A7R34, 1:50), CD135/Flt3 (A2F10.1), Flt3 (A2B10), Ly-6G/Gr1 (RB6-8C5), IgD (11-26c.2a), IgM (R6-60.2), *Sca1*/Ly6A/E (E13-161.7, 1:50), CD21 (7G6), CD22 (Lyb-8.2)(Cy34.1), CD23 (B3B4), CD25 (PC61), CD48 (HM48-1), CD150 (TC15-12F12.2) and Ter119 (TER119) antibodies. Unspecific antibody binding was suppressed by preincubation with CD16/CD32 (2.4G2) Fc-block solution (Pharmingen). The different haematopoietic progenitors and B-cell stages were defined by flow cytometry as shown in Supplementary Fig. 6. All antibodies were purchased from BD Biosciences. All antibodies were used at a 1:100 dilution unless otherwise indicated.

V(D)J recombination. Immunoglobulin rearrangements were amplified by PCR using the primers listed in Supplementary Table 4 (ref. 49). Cycling conditions consisted of an initial heat activation at 95 °C followed by 31–37 cycles of denaturation for 1 min at 95 °C, annealing for 1 min at 65 °C for heavy chains or 62 °C for light chains, and elongation for 1 min 45 s at 72 °C. This was followed by a final elongation for 10 min at 72 °C. To determine the DNA sequences of individual V(D)J rearrangements, the PCR fragments were isolated from the agarose gel and cloned into the pGEM-Teasy vector (Promega); the DNA inserts of at least 10 clones corresponding to the same PCR fragment were then sequenced.

Immunohistochemistry. Tissue samples were taken from homogenous portions of the resected organ by the pathologist and fixed immediately after excision. Samples of each organ were processed into paraffin, sectioned and examined histologically including routinely standard haematoxylin and eosin and immunohistochemical techniques. Transgenic mice samples were sectioned, dewaxed and heated in 10 mmol l⁻¹ sodium citrate buffer for 30 min. Slides were incubated with primary antibodies. The antibodies used included: *Bcl6* (N-3, Santa Cruz, 1:100); *Pax5* (C-20, Santa Cruz, 1:125), *CD21* (A-3, Santa Cruz, 1:125); and *IgG* (A85-I, BD Biosciences, 1:20). Samples were centrally reviewed by a panel of pathologists and diagnosed using uniform criteria based on clinical, histological, immunophenotypic and molecular characteristics. For comparative studies, age-matched mice were used.

Analysis of germinal centre formation. Sheep red blood cells (1–2 × 10⁸ cells) were injected into the peritoneum of control, *Sca1-Bcl6^{flox}* mice and *Sca1-Bcl6^d* mice. Ten days later, the spleens were analysed by immunohistochemistry. The spleens of control, *Sca1-Bcl6^{flox}* mice and *Sca1-Bcl6^d* mice were isolated, embedded in OCT compound (Sakura) and snap-frozen on dry ice. Cryosections of the spleen were stained with a FITC-anti-IgD antibody (1:100 dilution, BD Biosciences) and biotinylated PNA (1:100 dilution, clone B-1075, Vector Laboratories). FITC-anti-IgD was detected with an alkaline phosphatase-coupled anti-FITC antibody (Roche), which was visualized by incubation with Fast Red (Sigma). Biotinylated PNA was detected with horseradish peroxidase-conjugated streptavidin (Zymed) followed by incubation with diaminobenzidine (Sigma).

Pro-B cell culture. Iscove's modified Dulbecco's medium supplemented with 50 μM β-mercaptoethanol, 1 mM L-glutamine, 2% heat-inactivated fetal calf serum and 0.03% (w/v) primatone RL (Sigma) was used for Pro-B cell culture experiments. Pro-B cells isolated by magnetic-activated cell sorting for B220⁺ (Miltenyi Biotec) from bone marrow of 2-week-old mice were cultured on irradiated ST2 cells in Iscove's Modified Dulbecco's medium containing IL-7 (R&D Systems). The cells were maintain in culture for 1 week and then collected for Southern blot experiments.

Gene expression microarray analysis of murine tumours. Tumour-bearing spleens were harvested from *Sca1-Bcl6^{flox}* and *Sca1-Bcl6^d* mice, and healthy spleens were harvested from control mice; cells were not sorted before RNA extraction for this analysis. Total RNA was isolated in two steps using TRIzol (Life Technologies) followed by RNeasy Mini-Kit (Qiagen) purification following the manufacturer's RNA Clean-up protocol with the optional On-column DNase treatment. The integrity and the quality of the RNA were verified by electrophoresis and its concentration was measured. Samples were analysed using Affymetrix Mouse Genome 430 2.0 arrays. Data were normalized as described above, and data sets containing the WT and either the *Sca1-Bcl6^{flox}* or *Sca1-Bcl6^d* samples were filtered separately by median absolute deviation to derive the most variably expressed 10,000 genes for each comparison for use in GSEA and differential gene expression analysis. Differential gene expression analysis was performed using the *ComparativeMarkerSelection* module of GenePattern⁵⁹ with *T*-test statistic, and correcting for multiple hypothesis testing using 1,000 permutations. Genes were deemed to be significantly differentially expressed with a FDR *Q* value <0.25 and a fold change ≥ 1.25. Differentially expressed genes were tested for enrichment of genes associated with normal murine B-cell differentiation states. Gene expression signatures that are specifically upregulated in pre/pro-B cells, transitional B-cells, follicular or marginal zone B-cells, GCB cells, plasmablasts and plasma cells were assessed for their overlap with that were upregulated within tumour specimens using hypergeometric enrichment analysis^{29,30}. The relative over abundance of a specific differentiation state within a tumour sample compared with a WT spleen is therefore detected by significant enrichment of the signature that is definitive of that differentiation state.

DNA methylation profiling. *EpiQuest library construction:* EpiQuest libraries were prepared from 200 to 500 ng mouse genomic DNA obtained from primary cells (*Sca1*⁺ *Lin*⁻ cells from bone marrow, and B220⁺ cells and Gr1⁺ Mac1⁺ from peripheral blood) purified from *Sca1-Bcl6^d* mice and/or WT mice. DNA were pooled from 6 to 9 mice to provide one pooled replicate per condition, as performed previously^{64,65}. The DNA was digested with 60 units of TaqI and 30 units of MspI (New England Biolabs) sequentially. Size-selected TaqI-MspI fragments (40–120 bp and 120–350 bp) were filled in and 3'-terminal-A extended, extracted with a DNA Clean & Concentrator kit (Zymo Research). Ligation to pre-annealed adaptors containing 5-methyl-cytosine (5 mC) instead of cytosine was performed using the Illumina DNA preparation kit and protocol. Purified, adaptor-ligated fragments were bisulphite-treated using the EZ DNA Methylation-Direct Kit (Zymo Research). Preparative-scale PCR (18 cycles) was performed and purified PCR products were subjected to a final size selection on a 4% NuSieve 3:1 agarose gel. SYBR-green-stained gel slices containing adaptor-ligated fragments of 130–210 bp or 210–460 bp in size were excised. Library material was recovered from the gel using a Zymoclean Gel DNA Recovery Kit (Zymo Research) and sequenced on an GAIIX genome analyzer (Illumina), yielding between 43,930,708 and 60,139,994 total reads for each condition.

Sequence alignments and data analysis: Sequence reads from bisulphite-treated EpiQuest libraries were identified using standard Illumina base-calling software and then analysed using a Zymo Research proprietary computational pipeline. Residual Cs in each read were first converted to thymines (Ts), with each such conversion noted for subsequent analysis. A reference sequence database was constructed from the 36-bp ends of each computationally predicted *MspI*-*TaqI* fragment in the 40–220-bp size range. All Cs in each fragment end were then converted to thymines. (Only the C-poor strands are sequenced in the reduced representation bisulfite sequencing process.) The converted reads were aligned to the converted reference by finding all 12-bp perfect matches and then extending to both ends of the treated read, not allowing gaps (reverse complement alignments were not considered). The number of mismatches in the induced alignment was then counted between the unconverted read and reference, ignoring cases in which a T in the unconverted read is matched to a C in the unconverted reference. For a given read, the best alignment was kept if the second-best alignment had two more mismatches; otherwise the read was discarded as non-unique. The mean CpG coverages ranged between 5–11X and total number of unique mapped reads ranged between 3,378,764 and 10,295,957 for each condition. The methylation level of each sampled C was estimated as the number of reads reporting a C, divided by the total number of reads reporting a C or T. A bioinformatics pipeline was used to score epigenetic alterations according to strength and significance, and links them to potentially affected genes. To that end, we collected a comprehensive set of regions of interest, which includes promoters, CpG islands and repetitive elements. For each of these regions, the number of methylated and unmethylated CpG observations is determined, and a *P* value is assigned using Fisher's exact test. Once all *P* values are calculated, multiple-testing correction is performed separately for

each region type using the Q value method, which controls the FDR to be below a user-specified threshold (typically 10%). The software pipeline is implemented in Python (alignment processing module) and R (statistical analysis module). Unsupervised clustering was performed on methylation ratio data from each condition using Kendall tau rank correlation.

Exome sequencing. Next-generation sequencing libraries were prepared using NEBnext DNA sample prep kit (New England Biolabs) and exome capture performed using SureSelect XT Mouse All Exon (Agilent). Sequencing was performed using Genome Analyzer II instrument (Illumina) with 75 bp paired-end reads, and one sample per lane. Raw sequences were trimmed by 2 bp at their 5' ends to remove GC bias, and aligned to the murine genome (mm9) using Burrows-Wheeler Aligner with default parameters⁶⁶. Somatic mutations and DNA copy number alterations were called with reference to age- and gender-matched controls using VarScan 2.0 (ref. 67). Somatic nucleotide variants were discarded if they (i) did not have a significant *P* value ($P \leq 0.05$) determined by VarScan 2.0; (ii) were not determined to be somatic alterations by VarScan 2.0; (iii) were present in $\geq 10\%$ of reads within the control sample; (iv) were not observed in both strands during sequencing; and (v) were not in the coding region of a gene.

Bone marrow transplantation experiments. In order to determine the nature of the lymphomagenic cell, bone marrow transplantation experiments were performed. BM LSK or splenic B220⁺ cells were isolated and highly purified from either male *Sca1-Bcl6*^d (C57BL/6 \times CBA) or male WT mice (C57BL/6 \times CBA). Mice were 12 months old. The sorting purity of these cells was analysed by FACS and determined to be over 98%. In each cohort, these cells were injected intravenously into sublethally irradiated (4 Gy) secondary recipient 12-week-old male syngenic mice (C57BL/6 \times CBA). Diseased recipient mice were killed and assessed for B-cell lymphoma development.

Bcl6 DNA-binding sequence motif analysis. DNA sequences were obtained for genomic regions that were (i) significantly hypermethylated in both HSPCs and mature B-cells from *Sca1-Bcl6*^d mice compared with identical populations from WT mice; (ii) significantly hypomethylated in both HSPCs and mature B-cells from *Sca1-Bcl6*^d mice compared with identical populations from WT mice; and (iii) were not differentially methylated between *Sca1-Bcl6*^d mice populations and those from WT mice (Supplementary Data 3). Genomic regions were searched for BCL6 DNA-binding sequence motifs (5'-TTTNNGNATCTTT-3') (ref. 68) using the CisFinder⁶⁹ identify motifs function, with an FDR of 0.2 and a matching threshold of 0.75.

References

- Alizadeh, A. *et al.* Distinct types of diffuse large B-cell lymphoma identified by gene expression profiling. *Nature* **403**, 503–511 (2000).
- Morin, R. *et al.* Frequent mutation of histone-modifying genes in non-Hodgkin lymphoma. *Nature* **476**, 298–303 (2011).
- Pasqualucci, L. *et al.* Inactivating mutations of acetyltransferase genes in B-cell lymphoma. *Nature* **471**, 189–195 (2011).
- Shaffer, A., Young, R. & Staudt, L. Pathogenesis of human B cell lymphomas. *Annu. Rev. Immunol.* **30**, 565–610 (2012).
- Chaganti, S. *et al.* Involvement of BCL6 in chromosomal aberrations affecting band 3q27 in B-cell non-Hodgkin's lymphoma. *Genes Chromosomes Cancer* **23**, 323–327 (1998).
- Ye, B. *et al.* Alterations of a zing finger-encoding gene, BCL-6, in diffuse large B-cell lymphoma. *Science* **262**, 747–750 (1993).
- Bihui, H. *et al.* The BCL-6 proto-oncogene controls germinal-centre formation and Th2-type inflammation. *Nat. Genet.* **16**, 161–170 (1997).
- Dent, A., Shaffer, A., Yu, X., Allman, D. & Staudt, L. Control of inflammation, cytokine expression, and germinal center formation by BCL-6. *Science* **276**, 589–592 (1997).
- Lossos, I. *et al.* Expression of a single gene, BCL-6, strongly predicts survival in patients with diffuse large B-cell lymphoma. *Blood* **98**, 945–951 (2001).
- Lossos, I., Akasaka, T., Martinez-Climent, J., Siebert, R. & Levy, R. The BCL6 gene in B-cell lymphomas with 3q27 translocations is expressed mainly from the rearranged allele irrespective of the partner gene. *Leukemia* **17**, 1390–1397 (2003).
- Duy, C. *et al.* BCL6 enables Ph⁺ acute lymphoblastic leukaemia cells to survive BCR-ABL1 kinase inhibition. *Nature* **473**, 384–388 (2011).
- Hurtz, C. *et al.* BCL6-mediated repression of p53 is critical for leukemia stem cell survival in chronic myeloid leukemia. *J. Exp. Med.* **208**, 2163–2174 (2011).
- Weigert, O. & Weinstock, D. M. The evolving contribution of hematopoietic progenitor cells to lymphomagenesis. *Blood* **120**, 2553–2561 (2012).
- Green, M. *et al.* Hierarchy in somatic mutations arising during genomic evolution and progression of follicular lymphoma. *Blood* **121**, 1604–1611 (2013).
- Alizadeh, A. & Majeti, R. Surprise! HSC are aberrant in chronic lymphocytic leukemia. *Cancer Cell* **20**, 135–136 (2011).
- Jan, M. *et al.* Clonal evolution of preleukemic hematopoietic stem cells precedes human acute myeloid leukemia. *Sci. Transl. Med.* **4**, 149ra118 (2012).
- Kikushige, Y. *et al.* Self-renewing hematopoietic stem cell is the primary target in pathogenesis of human chronic lymphocytic leukemia. *Cancer Cell* **20**, 246–259 (2011).
- Welch, J. *et al.* The origin and evolution of mutations in acute myeloid leukemia. *Cell* **150**, 264–278 (2012).
- Weinstein, B. Addiction to oncogenes—the achilles heel of cancer. *Science* **297**, 63–64 (2002).
- Zack, T. *et al.* Pan-cancer patterns of somatic copy number alteration. *Nat. Genet.* **45**, 1134–1140 (2013).
- Green, M. *et al.* Integrative analysis reveals selective 9p24.1 amplification, increased PD-1 ligand expression, and further induction via JAK2 in nodular sclerosing Hodgkin lymphoma and primary mediastinal large B-cell lymphoma. *Blood* **116**, 3268–3277 (2010).
- Basso, K. & Dalla-Favera, R. Roles of BCL6 in normal and transformed germinal center B-cells. *Immunol. Rev.* **247**, 172–183 (2012).
- Lenz, G. *et al.* Molecular subtypes of diffuse large B-cell lymphoma arise by distinct genetic pathways. *Proc. Natl Acad. Sci. USA* **105**, 13520–13525 (2008).
- Iqbal, J. *et al.* Distinctive patterns of BCL6 molecular alterations and their functional consequences in different subgroups of diffuse large B-cell lymphoma. *Leukemia* **21**, 2332–2343 (2007).
- Basso, K. *et al.* Integrated biochemical and computational approach identifies BCL6 direct target genes controlling multiple pathways in normal germinal center B cells. *Blood* **115**, 975–984 (2010).
- Laurenti, E. *et al.* The transcriptional architecture of early human hematopoiesis identifies multilevel control of lymphoid commitment. *Nat. Immunol.* **14**, 756–763 (2013).
- Shay, T. *et al.* Conservation and divergence in the transcriptional programs of the human and mouse immune systems. *Proc. Natl Acad. Sci. USA* **110**, 2946–2951 (2013).
- Miles, C., Sanchez, M. J., Sinclair, A. & Dzierzak, E. Expression of the Ly-6E.1 (Sca-1) transgene in adult hematopoietic stem cells and the developing mouse embryo. *Development* **124**, 537–547 (1997).
- Green, M. *et al.* Signatures of murine B-cell development implicate Yy1 as a regulator of the germinal center-specific program. *Proc. Natl Acad. Sci. USA* **108**, 2873–2878 (2011).
- Romero-Camarero, I. *et al.* Germinal center protein HGAL promotes lymphoid hyperplasia and amyloidosis via BCR-mediated Syk activation. *Nat. Commun.* **4**, 1338 (2013).
- Adams, J. & Strasser, A. Is tumor growth sustained by rare cancer stem cells or dominant clones. *Cancer Res.* **68**, 4018–4021 (2008).
- Monti, S. *et al.* Integrative analysis reveals an outcome-associated and targetable pattern of p53 and cell cycle deregulation in diffuse large B cell lymphoma. *Cancer Cell* **22**, 359–372 (2012).
- Raynal, N. *et al.* DNA methylation does not stably lock gene expression but instead serves as a molecular mark for gene silencing memory. *Cancer Res.* **72**, 1170–1181 (2012).
- Nowell, P. The clonal evolution of tumor cell populations. *Science* **194**, 23–28 (1996).
- Huntlet, B. & Gilliland, D. Leukaemia stem cells and the evolution of cancer stem cell research. *Nat. Rev. Cancer* **5**, 311–321 (2005).
- Hart, J. *et al.* Transmission of a follicular lymphoma by allogeneic bone marrow transplantation—evidence to support the existence of lymphoma progenitor cells. *Br. J. Haematol.* **136**, 163–172 (2006).
- Pasqualucci, L. *et al.* Mutations of the BCL6 proto-oncogene disrupts its negative auto-regulation in diffuse large B-cell lymphoma. *Blood* **101**, 2914–2923 (2003).
- Dent, A., Vanaswala, F. & Toney, L. Regulation of gene expression by the proto-oncogene BCL-6. *Crit. Rev. Oncol. Hematol.* **41**, 1–9 (2002).
- Chung, Y. *et al.* Follicular regulatory T cells expressing Foxp3 and Bcl-6 suppress germinal center reactions. *Nat. Med.* **17**, 983–988 (2011).
- Nurieva, R. *et al.* Bcl6 mediates the development of T follicular helper cells. *Science* **325**, 1001–1008 (2009).
- Ichii, H. *et al.* Role for Bcl-6 in the generation and maintenance of memory CD8⁺ T cells. *Nat. Immunol.* **3**, 558–563 (2002).
- Toney, L. *et al.* BCL-6 regulates chemokine gene transcription in macrophages. *Nat. Immunol.* **1**, 214–220 (2000).
- Phan, R. & Dalla-Favera, R. The BCL6 proto-oncogene suppresses p53 expression in germinal-center B cells. *Nature* **432**, 635–639 (2004).
- Cattoretti, *et al.* Deregulated BCL6 expression recapitulates the pathogenesis of human diffuse large B cell lymphoma in mice. *Cancer Cell* **7**, 445–455 (2005).
- Ruminy, P. *et al.* The isotype of the BCR as a surrogate for the GCB and ABC molecular subtypes in diffuse large B-cell lymphoma. *Leukemia* **25**, 681–688 (2011).
- Lenz, G. *et al.* Aberrant immunoglobulin class switch recombination and switch translocations in activated B cell-like diffuse large B cell lymphoma. *J. Exp. Med.* **204**, 633–643 (2007).

47. Lossos, I. *et al.* Ongoing immunoglobulin somatic mutation in germinal center B cell-like but not in activated B cell-like diffuse large cell lymphomas. *Proc. Natl Acad. Sci. USA* **97**, 10209–10213 (2000).
48. Thieblemont, C. *et al.* The germinal center/activated B-cell subclassification has a prognostic impact for response to salvage therapy in relapsed/refractory diffuse large B-cell lymphoma: A Bio-CORAL study. *J. Clin. Oncol.* **29**, 4079–4087 (2011).
49. Jain, M. *et al.* Sustained loss of a neoplastic phenotype by brief inactivation of MYC. *Science* **297**, 102–104 (2002).
50. Tsai, A. *et al.* Human chromosomal translocations at CpG sites and a theoretical basis for their lineage and stage specificity. *Cell* **135**, 1130–1142 (2008).
51. Compagno, M. *et al.* Mutations of multiple genes cause deregulation of NF- κ B in diffuse large B-cell lymphoma. *Nature* **459**, 717–720 (2009).
52. Davis, R. *et al.* Chronic active B-cell-receptor signalling in diffuse large B-cell lymphoma. *Nature* **463**, 88–92 (2010).
53. Cerchiotti, L. *et al.* A peptomimetic inhibitor of BCL6 with potent antilymphoma effects *in vitro* and *in vivo*. *Blood* **113**, 3397–3405 (2009).
54. Scandurra, M. *et al.* Genomic lesions associated with a different clinical outcome in diffuse large B-Cell lymphoma treated with R-CHOP-21. *Br. J. Haematol.* **151**, 221–231 (2010).
55. Green, M. *et al.* Integrative genomic profiling reveals conserved genetic mechanisms for tumorigenesis in common entities of non-Hodgkin's lymphoma. *Genes Chromosomes Cancer* **50**, 313–326 (2011).
56. Kato, M. *et al.* Frequent inactivation of A20 in B-cell lymphomas. *Nature* **459**, 712–716 (2009).
57. Mermel, C. *et al.* GISTIC2.0 facilitates sensitive and confident localization of the targets of focal somatic copy-number alteration in human cancers. *Genome Biol.* **12**, R41 (2011).
58. Brune, V. *et al.* Origin and pathogenesis of nodular lymphocyte—predominant Hodgkin lymphoma as revealed by global gene expression analysis. *J. Exp. Med.* **205**, 2251–2268 (2008).
59. Reich, M. *et al.* GenePattern 2.0. *Nat. Genet.* **38**, 500–501 (2006).
60. Johnson, W., Rabinovic, A. & Li, C. Adjusting batch effects in microarray expression data using Empirical Bayes methods. *Biostatistics* **8**, 118–127 (2007).
61. Wright, G. *et al.* A gene expression-based method to diagnose clinically distinct subgroups of diffuse large B cell lymphoma. *Proc. Natl Acad. Sci. USA* **100**, 9991–9996 (2003).
62. Subramanian, A., Kuehn, H., Gould, J., Tamayo, P. & Mesirov, J. GSEA-P: a desktop application for Gene Set Enrichment Analysis. *Bioinformatics* **23**, 3251–3253 (2007).
63. Jacks, T. *et al.* Tumor spectrum analysis in p53-mutant mice. *Curr. Biol.* **4**, 1–7 (1994).
64. Taylor, K. *et al.* Ultra-deep bisulfite sequencing analysis of DNA methylation patterns in multiple gene promoters by 454 sequencing. *Cancer Res.* **67**, 8511–8518 (2007).
65. Seisenberger, S. *et al.* The dynamics of genome-wide DNA methylation reprogramming in mouse primordial germ cells. *Mol. Cell* **48**, 849–862 (2012).
66. Li, H. & Durbin, R. Fast and accurate long-read alignment with Burrows-Wheeler transform. *Bioinformatics* **26**, 589–595 (2010).
67. Koboldt, D. *et al.* VarScan 2: Somatic mutation and copy number alteration discovery in cancer by exome sequencing. *Genome Res.* **22**, 568–576 (2012).
68. Baron, B. *et al.* BCL6 encodes a sequence-specific DNA binding protein. *Genes Chromosomes Cancer* **13**, 332–224 (2003).
69. Sharov, A. & Ko, M. Exhaustive search for over-represented DNA sequence motifs with CisFinder. *DNA Res.* **16**, 261–273 (2009).

Acknowledgements

We are grateful to Dr Meinrad Busslinger for continuous and generous help and ideas over the years with this project, Dr Takeshi Tokuhisa for the mouse Bcl6 cDNA, Professor Michael Reth for the mb1-cre mice and Dr E. Dzierzak for the Sca1 promoter. Research in A.A.A. group is supported in part by the Damon Runyon Cancer Research Foundation, the Lymphoma Research Foundation, Gabrielle's Angel Foundation for Cancer Research, the Leukemia and Lymphoma Society, the National Institutes of Health, and the Department of Defense. Research in I.S.-G. group is supported partially by FEDER and by MICINN (SAF2009-08803 and SAF2012-32810), Junta de Castilla y León (CSI13A08 and proyecto Biomedicina 2009–2010), MEC OncoBIO Consolider-Ingenio 2010 (ref. no. CSD2007-0017), National Institutes of Health (NIH) grant (R01 CA109335-04A1) and by Group of Excellence Grant (GR15) from Junta de Castilla y León. M.R.G. and A.A.A. are Special Fellows of the Leukemia and Lymphoma Society. Funding for single-cell human HSPC studies was provided by NIH grant (U01HL099999) to R.M. and A.A.A. A.M. is supported by NCI R01 CA104348, the Chemotherapy Foundation, the Sam Waxman Cancer Research Foundation, and the G&P Foundation, and is a Leukemia and Lymphoma Society Scholar. Research at C.C.'s lab is partially supported by FEDER, Fondo de Investigaciones Sanitarias (PI080164), Proyectos Intramurales Especiales (CSIC) and Junta de Castilla y León (SA060A09 and proyecto Biomedicina 2009–2010). Research of A.O. is supported by a grant from the Instituto de Salud Carlos III, Ministerio de Sanidad y Consumo, Madrid, Spain (IISCIII-RTICC RD06/0020/0035-FEDER).

Author contributions

M.R.G. and C.V.-D. designed and conducted the majority of experiments, analysed the data and wrote the manuscript; M.R.G., A.A.A., I.R.-C., B.D. C.L.L., I.G.-H., E.A.-E., E.C.-S., R.J., J.A.M.-C., F.J.G.C., M.B.G.C., S.Z., Y.N., I.S.L., A.M., R.M. and C.C. performed experiments and analysed the data; B.P. generated Bcl6-floxed mice, and I.G.-R. characterized the Bcl6-floxed and p53 mutant mice; A.O. analysed flow cytometry data; T.F. and O.B. prepared tissue sections and helped to analyse mouse histopathology; S.Z. and Y.N. performed immunohistochemical characterization of mouse tissues; Y.N. provided expert classification of DLBCL tumours as a trained haematopathologist; J.I. and W.C.C. provided primary human DLBCL tumour BCL6 genotypes and corresponding gene expression profiles. A.A.A. and I.S.-G. conceived the project, designed the research, analysed the data, prepared the manuscript, and contributed equally as senior authors in supervising and funding the project. All authors commented upon and edited the final manuscript.

Additional information

Data accession numbers: Gene expression omnibus accession number for data in this study are as follows. DNA copy number data; GSE11318, GSE12906, GSE15127, GSE22082, GSE34171. Gene expression microarray data from from DLBCL tumors and normal B-cells; GSE11318, GSE34171, GSE12453. Data produced by this study; GSE36503, GSE56310.

Supplementary Information accompanies this paper at <http://www.nature.com/naturecommunications>

Competing financial interests: The authors declare no competing financial interests.

Reprints and permission information is available online at <http://npg.nature.com/reprintsandpermissions/>

How to cite this article: Green, M. R. *et al.* Transient expression of Bcl6 is sufficient for oncogenic function and induction of mature B-cell lymphoma. *Nat. Commun.* 5:3904 doi: 10.1038/ncomms4904 (2014).